JOURNAL OF VIROLOGY, Dec. 1990, p. 6110–6120
0022-538X/90/126110-11$02.00/0

Vol. 64, No. 12

Analysis of the Role of Brome Mosaic Virus 1a Protein Domains in RNA Replication, Using Linker Insertion Mutagenesis

PHILIP A. KRONER,† BENJAMIN M. YOUNG,‡ AND PAUL AHLQUIST*

Institute for Molecular Virology and Department of Plant Pathology, University of Wisconsin—Madison, Madison, Wisconsin 53706

Received 15 June 1990/Accepted 5 September 1990

Brome mosaic virus (BMV) belongs to a "superfamily" of plant and animal positive-strand RNA viruses that share, among other features, three large domains of conserved sequence in nonstructural proteins involved in RNA replication. Two of these domains reside in the 109-kDa BMV 1a protein. To examine the role of 1a, we used biologically active cDNA clones of BMV RNA1 to construct a series of linker insertion mutants bearing two-codon insertions dispersed throughout the 1a gene. The majority of these mutations blocked BMV RNA replication in protoplasts, indicating that both intervirally conserved domains function in RNA replication. Coinoculation tests with a large number of mutant combinations failed to reveal detectable complementation between mutations in the N- and C-terminal conserved domains, implying that these two domains either function in some directly interdependent fashion or must be present in the same protein. Four widely spaced mutations with temperature-sensitive (*ts*) defects in RNA replication were identified, including a strongly *ts* insertion near the nucleotide-binding consensus of the helicaselike C-terminal domain. Temperature shift experiments with this mutant show that 1a protein is required for continued accumulation of all classes of viral RNA (positive strand, negative strand, and subgenomic) and is required for at least the first 10 h of infection. *ts* mutations were also identified in the 3′ noncoding region of RNA1, 5′ to conserved sequences previously implicated in *cis* for replication. Under nonpermissive conditions, the *cis*-acting partial inhibition of RNA1 accumulation caused by these noncoding mutations was also associated with reduced levels of the other BMV genomic RNAs. Comparison with previous BMV mutant results suggests that RNA replication is more sensitive to reductions in expression of 1a than of 2a, the other BMV-encoded protein involved in replication.

Brome mosaic virus (BMV), type member of the plant bromovirus group, is an icosahedral positive-strand RNA virus that infects mainly monocots, including barley, wheat, and many grasses (30). The 8.2-kb BMV genome is divided among three RNAs designated RNA1 (3.2 kb), RNA2 (2.9 kb), and RNA3 (2.1 kb) whose sequences are known (3, 5). RNAs 1 and 2 are monocistronic and serve as mRNAs for the nonstructural 1a (104-kDa) and 2a (94-kDa) proteins, while RNA3 is dicistronic, serving as the mRNA for the 32-kDa 3a protein and as a template for the production of subgenomic RNA4, the 20-kDa coat protein mRNA. While all three BMV genomic RNAs are required for systemic infection of whole plants (4), only RNAs 1 and 2 and their encoded proteins are necessary for viral RNA replication in isolated plant protoplasts (14, 27, 43).

Three large domains of sequence similarity exist between the 1a and 2a proteins of BMV and the nonstructural proteins implicated in the RNA replication of several plant viruses and animal alphaviruses such as Sindbis virus (6, 12, 15, 20). Despite dissimilar genetic organization, these viruses share certain features of replication, including production of capped viral RNAs and expression of genes via subgenomic RNAs. Conservation of these features suggests that these viruses utilize common replication strategies and implies that their related nonstructural proteins may share functions important for RNA-dependent RNA replication.

Accumulating evidence suggests that the 2a protein is a core polymerase for BMV replication. Kamer and Argos (26) identified amino acid motifs within the 2a protein and its homologs that are also present in several known RNA-dependent RNA polymerases. Single amino acid substitutions in one of these motifs (Gly-Asp-Asp) in the Qβ replicase β subunit all blocked replication, and the mutant proteins exhibited *trans*-dominant inhibition of wild-type (wt) phage replication (23). Recently we introduced a number of single-amino-acid substitutions into a different conserved region of the BMV 2a protein and recovered phenotypes that are consistent with 2a functioning in RNA chain elongation in addition to influencing template selection (28). Similar results were obtained by analysis of Sindbis virus mutants, in which mutations producing defects in RNA chain elongation (8) as well as in regulation of negative-strand synthesis (38) were mapped to the 2a-like nonstructural protein, nsP4.

Although such results have begun to clarify the role of the 2a protein in RNA replication, important fundamental questions remain about the role of the 1a protein. For example, 1a contains N- and C-terminal conserved domains that correspond, respectively, to the separate Sindbis proteins nsP1 and nsP2 (6). Do both of these 1a domains function in RNA replication? If so, will mutations in these domains have obviously separable phenotypes, and will deleterious mutations in either domain complement one another? Are 1a functions involved at all stages or only specific stages or pathways of the replication cycle?

To further characterize the participation of the BMV 1a protein in RNA replication and to investigate the functional relationship between the two conserved domains, we constructed a series of two-codon insertions in the 1a gene and analyzed their effect on BMV replication in barley proto-

* Corresponding author.
† Present address: The Blood Center of Southeastern Wisconsin, 1701 West Wisconsin Ave., Milwaukee, WI 53233.
‡ Present address: Tumor Biology Dept., Schering-Plough Research, Bloomfield, NJ 07003.

plasts at permissive and nonpermissive temperatures. Our results show that the 1a protein is indispensable for the synthesis of all classes of viral RNA and is required for at least the first 10 h after inoculation of plant protoplasts. Both of the conserved 1a protein domains were found to be involved in RNA replication, and complementation analyses revealed that the function of these domains is not completely independent.

MATERIALS AND METHODS

Materials. Plasmids pB1TP3, pB2TP5, and pB3TP8 contain complete cDNA copies of wt BMV RNAs 1, 2, and 3, respectively, and allow the in vitro synthesis of infectious BMV transcripts (4, 25). Plasmid pB1TP1 contains the complete cDNA sequence of BMV RNA1 and is identical to pB1TP3 except that it contains one extra guanine nucleotide at the 5′ end; transcripts from this plasmid are also infectious (25). Plasmids pUC4KAPA and pUC4KSAC and the linker dGGGCCC were obtained from Pharmacia P-L Biochemicals, Inc., Piscataway, N.J.

Mutant construction. Two-codon insertions were constructed by following the approach of Barany (7), with the modifications described below. Plasmid pB1TP1 was used for mutagenesis at *Taq*I restriction sites, and pB1TP3 was used for all other constructions. Partial restriction enzyme digestions of pB1TP1 or pB1TP3 were performed in the presence of 50 μg of ethidium bromide per ml, and linearization for each restriction enzyme was optimized by adjusting the enzyme concentration. Linearization was monitored by electrophoresis in 1% agarose gels with Tris-borate buffer (32). Linearized plasmids produced by *Rsa*I and *Alu*I digestion and plasmids linearized with *Hin*fI that were filled in with Klenow DNA polymerase (Boehringer-Mannheim Biochemicals, Indianapolis, Ind.) were ligated to a 6-base phosphorylated linker containing the *Apa*I restriction site (GGGCCC). After digestion with *Apa*I, linear plasmids were separated from linkers by electrophoresis in 1% low-melting-point agarose gels, purified by phenol extraction and ethanol precipitation, and ligated to the Kan^r gene fragment released by *Apa*I from pUC4KAPA. After transformation into *Escherichia coli* JM101, successful ligations were selected for on media containing kanamycin and ampicillin (50 μg/ml each). Individual transformants were screened by restriction analysis to determine the site of the insertion and to ensure that no small restriction fragments were lost. To remove the Kan^r gene cassette, selected clones were digested with *Apa*I and religated, resulting in a 6-base insertion. *Hin*fI mutant pB1PK16 contains a 9-base insertion, the result of filling in the ends of the linearized DNA with Klenow polymerase prior to ligation with the *Apa*I linker. Purified plasmids were again screened by restriction analysis to confirm the site of insertion and to ensure that no sequences were deleted or rearranged during construction.

A similar library of insertion mutants containing GGATCC insertions was created from plasmids linearized by partial digestion with *Taq*I, *Hin*PI, *Hpa*II, or *Mae*II, also in the presence of ethidium bromide. Following digestion, ends were filled in with Klenow DNA polymerase and ligated to the Kan^r gene removed from pUC4KSAC by *Bam*HI, which also had ends filled in with Klenow DNA polymerase. Screening to identify the size of insertion and removal of the Kan^r gene to create the 6-base insertion was as described above.

Plasmid pB1PK22 was constructed by linearizing linker insertion mutant pB1PK8 with *Bam*HI, filling in the ends with Klenow DNA polymerase, and then religating to create an additional 4-base insertion. Plasmid pB1PK23 was constructed by digesting pB1TP3 with *Xho*I and then treating the linear DNA with mung bean nuclease (Epicentre Technologies, Madison, Wis.) to create blunt ends. Religation created a 4-base deletion. The base changes in pB1PK8, pB1PK22, and pB1PK23 were confirmed by sequencing.

To confirm that frameshift mutations were not introduced into the 1a gene during mutant construction, RNA produced from the mutant plasmids by transcription with T7 RNA polymerase (New England BioLabs, Beverly, Mass.) was translated in vitro in the presence of [^{35}S]methionine (Amersham Corp., Arlington Heights, Ill.) by using a reticulocyte lysate extract (Promega, Madison, Wis.) and analyzed by sodium dodecyl sulfate-polyacrylamide gel electrophoresis (29).

RNA analysis. In vitro transcription, barley protoplast isolation and inoculation, RNA isolation, and Northern (RNA) blot analysis were performed as described by Kroner et al. (28). Typically, 1.0×10^5 protoplasts were inoculated with BMV transcripts in the presence of polyethylene glycol and $CaCl_2$ and then incubated in 1.5-ml microcentrifuge tubes in glass-covered water baths at either 24 or 35°C under fluorescent lighting (30 microeinsteins/m^2 s^{-1}) for 20 h, except where noted. After total RNA was isolated, the RNA equivalent to 1.0×10^4 inoculated protoplasts was separated by electrophoresis on 1% agarose gels and then transferred to Hybond nylon membrane (Amersham). For detection of negative-strand RNA, total protoplast RNA was denatured in the presence of glyoxal before electrophoresis. BMV positive- or negative-strand RNA was detected by hybridization to ^{32}P-labeled RNA transcribed from the appropriate strand of plasmid pB3HE1, which contains the 3'-terminal 200 nucleotides of RNA3, a sequence 97 to 99% conserved among all BMV RNAs (14). Hybridized RNA was visualized following exposure to Kodak XAR5 film (Eastman Kodak Co., Rochester, N.Y.) at −70°C with intensifying screens. The exposure required to visualize RNA varied between experiments because of differences in probe specific activity. For direct labeling experiments, 50 μCi of [5,6-^{3}H]uridine (Amersham) was added to inoculated cells. Total RNA was isolated and separated by electrophoresis in 1% nondenaturing agarose gels as described above. To visualize ^{3}H-labeled RNA, gels were treated with 1.0 M sodium salicylate for 30 min, dried under vaccuum, and exposed to Kodak XAR5 film at −70°C. Quantitative comments in this paper are based on densitometry of autoradiographs, which was performed with a Zeineh SLR-504-XL soft-laser scanning densitometer.

Filter hybridization. Filter hybridization based on the method of Maniatis et al. (32) was used to quantitate viral RNA synthesis in direct-labeling experiments. BMV RNA3 plasmid pB3TP8 was denatured in 0.5 N NaOH for 20 min at room temperature, and then 2-μl aliquots containing 10 μg of plasmid each were spotted directly onto Hybond nylon membrane. The membrane was allowed to air dry, and after incubation at 80°C for 15 min to enhance DNA binding, the membrane was neutralized in 100 ml of 2× SSC (0.3 M sodium chloride, 30 mM sodium citrate) for about 30 s and then rinsed twice in 100 ml of sterile deionized water. To remove loosely bound DNA, membranes were placed in 100°C sterile deionized water for 1 min, rinsed once in 100 ml of room temperature sterile deionized water, and then dried at room temperature. Individual spots (1 cm^2) containing denatured plasmid were cut from the membrane and transferred to microcentrifuge tubes. Prehybridization and hybridization with ^{3}H-labeled viral RNA for 24 h in 0.5 ml of

TABLE 1. Locations, names, and phenotypes of insertion mutations in BMV RNA1

pB1PKn mutant	Insertion		Inserted bases	Amino acid change[a]	Phenotype[b]
	Site	nt[c]			
1	*Taq*I	875	GGATCC	Ile-267–**Gly–Ser**–Asp-268	TS
2		1594	GGATCC	Ser-507–**Asp–Pro**–Lys-508	WT
3		89	GGATCC	Ile-5–**Gly–Ser**–Asp-6	—
4		1550	GGATCC	Phe-492–**Gly–Ser**–Asp-493	TS
5		695	GGATCC	Phe-207–**Gly–Ser**–Asp-208	WT
6		359	GGATCC	Leu-95–**Gly–Ser**–Asp-96	—
7		791	GGATCC	Phe-239–**Gly–Ser**–Asp-240	—
8		2990	GGATCC	**(3′ noncoding)**	TS
9		536	GGATCC	Phe-154–**Gly–Ser**–Asp-155	WT
10	*Rsa*I	667	GGGCCC	Val-198–**Gly–Pro**–Arg-199	—
11		683	GGGCCC	Gly-203–**Gly–Pro**–Thr-204	—
12		1008	GGGCCC	Lys-311–**Trp–Ala–His**–Val-313	—
13		1284	GGGCCC	Lys-403–**Trp–Ala–His**–Glu-405	—
14		1741	GGGCCC	Val-556–**Gly–Pro**–Pro-557	WT
15		2028	GGGCCC	Thr-651–**Trp–Ala–His**–Ile-653	—
16	*Hin*fI	1466	GGGCCCACT	Thr-464–**Gly–Pro–Thr**–Arg-465	—
17	*Mae*II	2680	GGATCC	Thr-869–**Asp–Pro**–Tyr-870	—
18		2810	GGATCC	Asn-912–**Gly–Ser**–Val-913	—
19	*Hin*PI	2084	GGATCC	Ser-670–**Gly–Ser**–Ala-671	TS
20		2788	GGATCC	Ala-905–**Asp–Pro**–Gln-906	—
21	*Hpa*II	1699	GGATCC	Pro-542–**Asp–Pro**–Val-543	WT

[a] Inserted amino acids are indicated by boldface. For mutants PK12, PK13, and PK15, the phase of the insertion led to an amino acid substitution adjacent to the two inserted amino acids, and the resultant altered amino acid is also shown in boldface.

[b] WT, RNA accumulation at 18, 24, and 35°C was equivalent to that of a wt infection; TS, RNA accumulation at 35°C was reduced relative to that at 24°C; —, no detectable RNA accumulation at 18, 24, or 35°C. See text for details.

[c] The insertion occurs after the indicated nucleotide (nt) in BMV RNA1.

hybridization solution was as described elsewhere (28), except that the hybridization temperature was 42°C. Removal of nonspecifically bound RNA was as described above for Northern blot analyses. The amount of [^{3}H]RNA bound to each filter was determined by liquid scintillation counting.

RESULTS

Construction and mapping of mutations in BMV RNA1. To investigate the role of the BMV 1a protein in RNA replication, 21 distinct linker insertions were constructed in biologically active BMV RNA1 cDNA clones (Table 1 and Fig. 1). Most of these mutants contain a 6-base insertion that, except for a single insertion in the 3′ noncoding region, results in the addition of two amino acids to the 1a protein. Insertions were targeted to the 4-base recognition sequences of six different restriction endonucleases, each with multiple sites within the 1a gene. Preferential cleavage of a subset of the available sites by each enzyme prevented recovery of mutants at all possible positions but nevertheless resulted in isolating insertions at locations spanning the entire 1a open reading frame (Fig. 1). The inserted sequences were chosen to introduce a unique restriction site into the BMV RNA1 cDNA to facilitate mapping and to provide useful sites for additional genetic manipulations. Fourteen mutants contained the 6-base *Bam*HI restriction site (GGATCC), which inserts a Gly-Ser or Asp-Pro into the 1a protein. Seven mutants contained the 6-base *Apa*I restriction site (GGGCCC), resulting in a Gly-Pro or Trp-Ala insertion. Three *Apa*I mutants contained a single-amino-acid substitution immediately adjacent to the 2-amino-acid insertion (Table 1). One *Apa*I mutant (PK16) contained a 9-base insertion resulting in the addition of three amino acids. Mutant plasmid constructs are named pB1PKn, where n identifies the individual mutant. For brevity, mutant transcripts produced in vitro and used for protoplast inoculations will be referred to as PKn. The sites of all insertions were verified by sequence analysis or restriction endonuclease mapping or both. The maintenance of the 1a open reading frame in each mutant was verified by translation of RNA in vitro followed by sodium dodecyl sulfate-polyacrylamide gel electrophoresis analysis (data not shown).

Identification of replication-defective phenotypes caused by insertions in 1a. The effects of the above-described amino acid insertions in the 1a protein on BMV RNA replication were examined in protoplasts isolated from 6-day-old barley plants. Protoplasts were inoculated with mixtures of transcripts from individual mutant RNA1 plasmids plus transcripts from wt RNA2 and RNA3 cDNA clones. After inoculation, infected protoplasts were divided into aliquots and incubated at 24 or 35°C for 20 h. To obtain precise temperature control, incubations were performed in glass-covered water baths under constant illumination. Investigation of the temperature profile of BMV replication under these conditions determined that the highest temperature tolerated by protoplasts that consistently allowed BMV replication was 35°C. This temperature is in close agreement with the nonpermissive temperature (34°C) used in previous analyses, in which incubation was performed in air incubators with similar lighting (28). Following the isolation of total protoplast RNA, the extent of viral RNA amplification was determined by Northern blot methods using radioactive probes specific for the detection of BMV positive-strand or negative-strand RNA, and the extent of viral RNA amplification was measured by laser densitometry of autoradiographs. All tests were repeated three or more times, and consistent results were obtained.

Twelve insertion mutations prevented detectable BMV

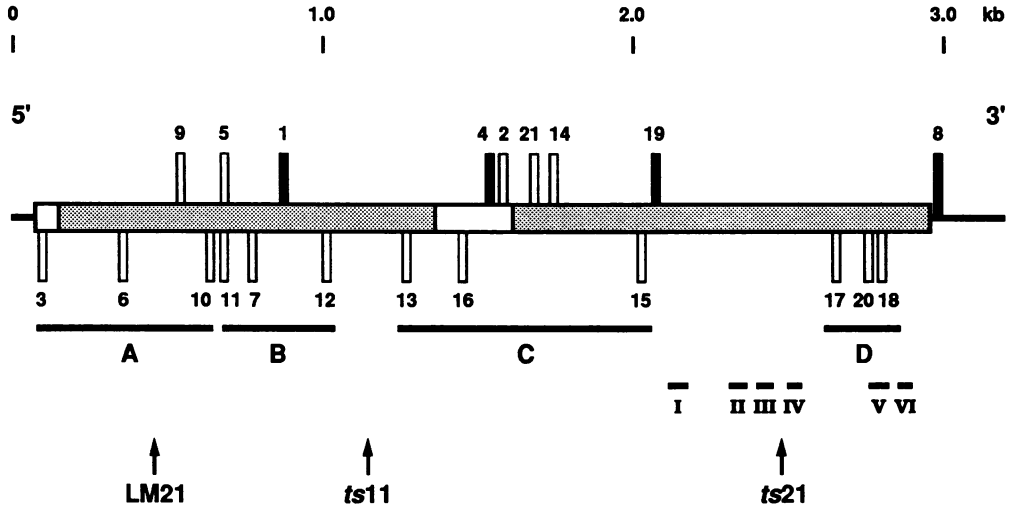

FIG. 1. Locations and phenotypes of insertion mutations in BMV RNA1. The central schematic represents BMV RNA1, with the large horizontal box representing the 1a protein open reading frame. The shaded areas within the box identify the two domains of the 1a protein sharing sequence similarity with other viral nonstructural proteins (6, 20). The RNA replication phenotypes of individual mutants were determined by Northern blot analysis of RNA isolated from infected barley protoplasts incubated at 24 or 35°C, as described in Materials and Methods. The positions of the insertion mutations and their phenotypes, as described in Table 1, are marked by vertical bars, with the number associated with each bar identifying the relevant mutant and its entry in Table 1. Bars pointing down represent lethal mutants. Bars pointing up represent viable mutants: clear bars above the open reading frame indicate mutants with phenotypes indistinguishable from that of wt BMV, and solid bars indicate mutants showing *ts* replication. Bars labeled A, B, C, and D identify the groups of lethal mutants used for complementation analyses as described in the text and presented in Fig. 5, and bars labeled I through VI indicate the six regions of the 1a C-terminal domain having sequence similarity with ATP-dependent helicases (21). Arrows at the bottom of the figure indicate the positions in the 1a protein that correspond to the sites of the three Sindbis virus mutants mapped to proteins nsP1 and nsP2 (see text).

replication (less than 0.2% of wt), as indicated by the absence of subgenomic RNA4 and genomic negative-strand RNA and the presence of genomic positive-strand RNA at extremely low levels no greater than the residual inoculum from nonreplicating transcript combinations lacking RNA1 or RNA2. (These behaviors are further documented below in the section on complementation results.) These lethal mutations are widely spaced throughout the 1a protein and are interspersed among mutations that have no detectable effect on BMV replication (Table 1 and Fig. 1). The inability of these lethal mutants to direct viral replication is most likely due to *trans*-acting defects in the 1a protein and not to *cis*-acting effects on RNA stability, as wt RNA1 and the lethal RNA1 mutants showed equivalent stability in inoculated protoplasts in the absence of replication (see, e.g., Fig. 5A). Although we cannot exclude the possibility that some of these insertions cause *cis*-acting replication defects, other analyses show that nonreplicating transcripts bearing a complete 1a open reading frame will direct low-level replication in protoplasts through transient expression of the 1a protein (P. Kroner, M. Janda, and P. Ahlquist, unpublished data). Thus, the lethal phenotypes of these mutations could not be due to *cis*-acting defects alone.

Eight other mutants with insertions in the 1a open reading frame were able to direct BMV replication in protoplasts at 24°C, indicating that the 1a protein can tolerate a number of insertions while still retaining some function. Infections directed at 24°C by six of these mutants (PK2, PK5, PK9, PK14, PK19, and PK21) were indistinguishable from infections containing wt RNA1 and accumulated normal levels of both positive- and negative-strand RNA (results not shown). Two mutants (PK1 and PK4) show reduced accumulation of viral RNA and altered RNA ratios compared with those caused by wt infections (Fig. 2). For mutant PK1, the overall accumulation of both positive- and negative-strand RNA at 24°C was reduced about fivefold compared with those in wt infections, and the level of PK1 RNA1 itself was selectively reduced an additional two- to threefold relative to genomic RNA2. For mutant PK4, positive-strand RNA accumulation was about 500-fold below wt levels, and the level of RNA4 was reduced relative to genomic RNAs 1 to 3 (Fig. 2). Negative-strand levels in PK4 infections were below the limit of detection.

To identify conditionally defective-replication phenotypes, protoplasts infected with mutant RNA were also incubated at 18 and 35°C as described above. Five mutants that showed wt levels of replication at 24°C also showed wt levels of replication at 35°C, while mutants PK1, PK4, and PK19 showed a substantial reduction in replication at the nonpermissive temperature (Fig. 2). For PK4 and PK19, no positive- or negative-strand RNA accumulation was detected at 35°C, while for PK1, positive-strand RNA accumulation at 35°C was reduced at least an additional 100-fold compared with that at 24°C. For all mutants, phenotypes in protoplasts incubated at 18°C were identical to those observed at 24°C, and mutants which failed to replicate at 24°C also failed to replicate at 35°C.

Temperature shift analyses of *ts* mutants PK1 and PK19. Time-course temperature shift analyses of *ts* mutants PK1 and PK19 were performed to identify when 1a functions are required in the virus replication cycle and to determine whether these mutants have specific defects in positive- or negative-strand synthesis. To carry out these experiments, it was first necessary to establish the kinetics of BMV RNA accumulation in wt infections of barley protoplasts grown at 24 and 35°C, so that shifts to 35°C could be made when both positive- and negative-strand RNAs were detectable and still accumulating. Protoplasts were inoculated with wt BMV

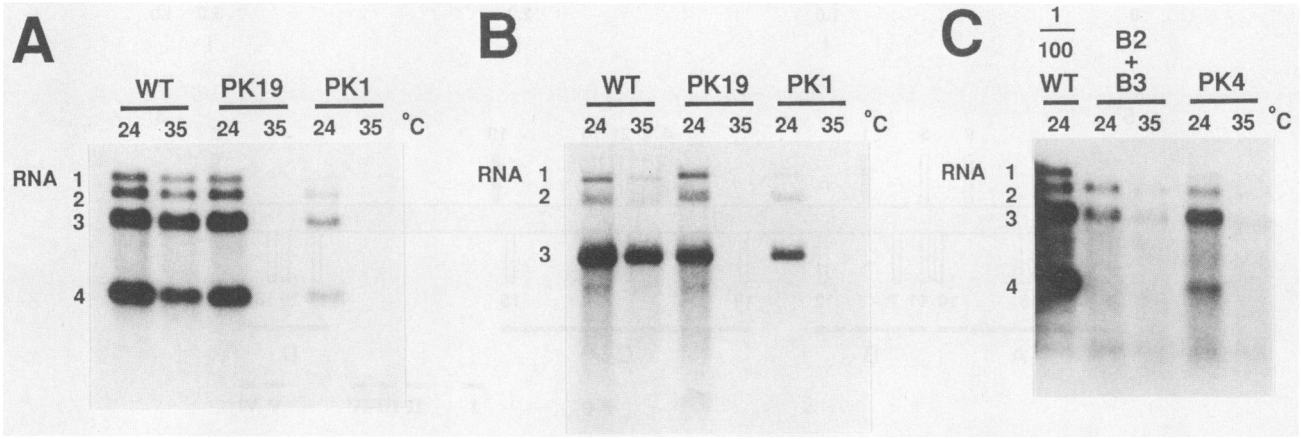

FIG. 2. Northern blot analysis of BMV RNA1 mutants with *ts* defects in RNA replication resulting from insertions within the 1a open reading frame. Transcripts from cDNA clones corresponding to wt RNA1 or the indicated RNA1 mutants were mixed with transcripts from wt BMV RNA2 (B2) and RNA3 (B3) cDNA clones and used to inoculate barley protoplasts. After incubation for 20 h at 24 or 35°C, total RNA was isolated and accumulation of viral positive-strand (A and C) and negative-strand (B) RNAs was determined by Northern blot techniques as described in Materials and Methods. PK4 negative-strand RNA levels were below the level of detection in these experiments and so are not illustrated in panel B. Each lane contains 1/10 of the total RNA extracted from 100,000 inoculated protoplasts, except for the WT lane labeled 1/100 in panel C, which contains 1/1,000 of the total RNA extracted from 100,000 inoculated protoplasts. The lanes labeled B2 + B3 in panel C were inoculated with wt BMV RNA2 and RNA3 transcripts alone. Autoradiograms were exposed for 1 h (A), 48 h (B), and 18 h (C).

transcripts and divided into multiple aliquots that were incubated at either 24 or 35°C. At each hour for the first 6 h postinoculation (p.i.) and at 8, 10, and 20 h p.i., total RNA was isolated from individual aliquots and viral RNA levels were determined by Northern blot analysis (left panels of Fig. 3A and 4A and results not shown). Similar results were obtained for cells incubated at 24 or 35°C, reflecting the fact that both temperatures are permissive for the wt BMV replicase. The first detectable accumulation of viral RNA, as determined by the appearance of subgenomic RNA4, oc-

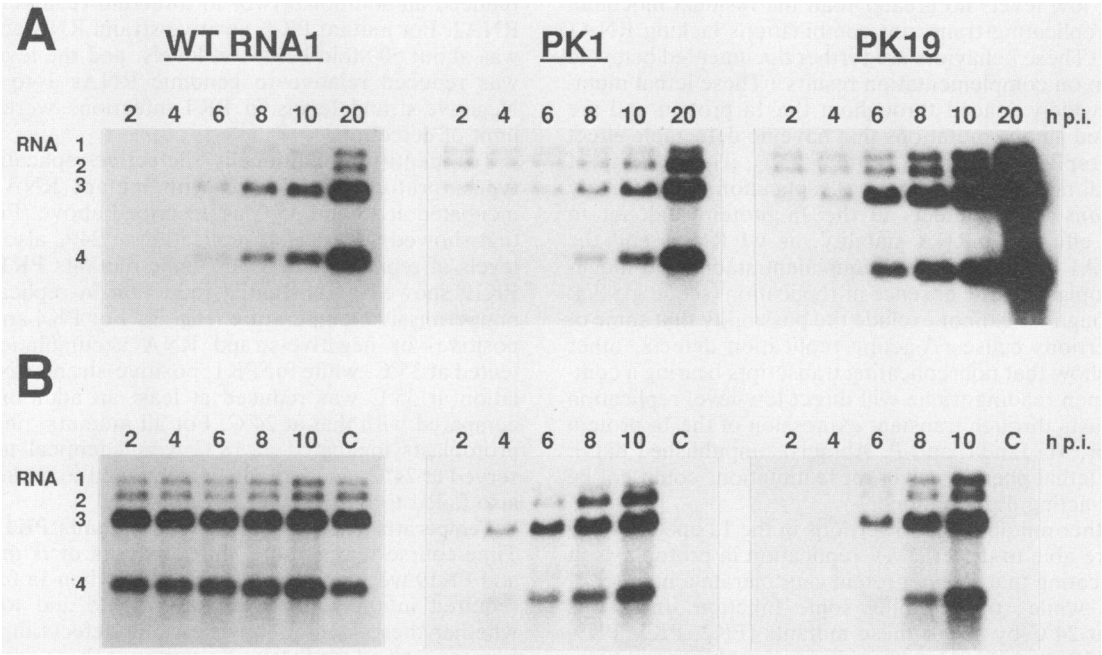

FIG. 3. Time-course temperature shift analysis of positive-strand viral RNA accumulation for wt BMV and *ts* mutants PK1 and PK19. (A) The number above each lane represents the number of hours p.i. that each aliquot was incubated at 24°C before isolation of total RNA. (B) The number above each lane represents the number of hours p.i. that each aliquot was incubated at 24°C prior to being shifted to 35°C. Thus, the amount of RNA detected for each protoplast aliquot in panel A represents the RNA present in the corresponding aliquots in panel B at the time of the shift to 35°C. The total incubation time for each aliquot in panel B was 20 h. Lanes C, Aliquots that were incubated continuously at 35°C for 20 h. Autoradiograms for wt were exposed for 2.5 h, and autoradiograms for PK1 and PK19 were exposed for 24 h.

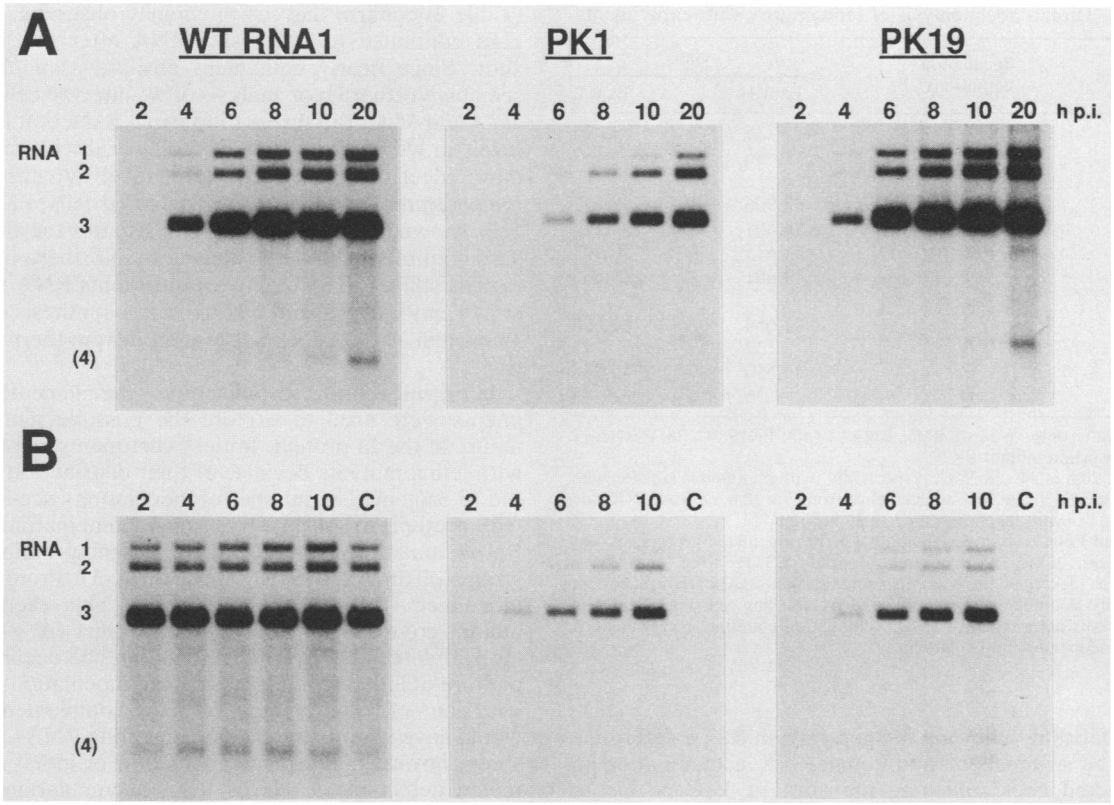

FIG. 4. Time-course temperature shift analysis of negative-strand viral RNA accumulation for wt BMV and *ts* mutants PK1 and PK19. RNA samples from the temperature shift experiment described in the legend to Fig. 3 were denatured in the presence of glyoxal, and negative-strand viral RNA was detected by Northern blot techniques as described in Materials and Methods. Labeling of each lane is as described in the legend to Fig. 3. All autoradiograms were exposed for 24 h.

curred 3 h p.i., with low levels of RNA continuing to accumulate through 10 h p.i. (Fig. 3A and longer exposures of similar experiments). The majority of positive-strand accumulation occurred from 10 to 20 h p.i., when the rate of accumulation was nearly linear. The pattern of negative-strand accumulation (Fig. 4A) differed from that of positive-strand RNA. The majority of negative-strand RNA accumulation occurred during the first 6 to 8 h p.i., and only a small further increase was detected from 10 to 20 h p.i.

For temperature shift analysis of wt RNA1 and *ts* mutants PK1 and PK19, 1.2×10^6 protoplasts were inoculated with the appropriate mutant or wt RNAs and divided into 12 aliquots. For each set of inoculations, one aliquot was incubated at 24°C and one was incubated at 35°C for the entire 20-h incubation period. Incubation of the remaining 10 aliquots of each set was initiated at 24°C. At 2, 4, 6, 8, and 10 h p.i., one of these aliquots was harvested for total RNA isolation and a separate aliquot was transferred to 35°C. At 20 h p.i., total RNA was isolated from all aliquots that had been shifted to 35°C and the viral RNA levels in each sample were determined by Northern blot analysis (Fig. 3 and 4).

For wt-infected cells, positive-strand RNA continued to accumulate in all aliquots after they were shifted from 24 to 35°C (Fig. 3A and B). However, a different pattern of negative-strand accumulation was observed (Fig. 4). Additional negative-strand RNA was synthesized in cells shifted to 35°C at 2 and 4 h p.i., but negative-strand RNA levels actually decreased in cells shifted at 6, 8, or 10 h p.i. These are times during which negative-strand RNA accumulation appeared to be reaching a plateau in cells incubated at 24°C (Fig. 4A and B).

The time course of both positive- and negative-strand RNA accumulation in PK19-infected cells at 24°C was similar to that seen for wt-infected cells (Fig. 3A and 4A). When PK19-infected cells were shifted to 35°C, though, no additional accumulation of positive- or negative-strand RNA was seen. RNA levels declined in all aliquots except the one shifted at 10 h p.i. In this aliquot, positive-strand levels were maintained at the 10-h p.i. level (Fig. 3 and 4).

For PK1-infected cells, the time course of RNA accumulation at 24°C was delayed compared with that of wt-infected cells, resulting in an overall reduction in the accumulation of both positive- and negative-strand RNA at 20 h p.i. (Fig. 3A and 4A). Perhaps because of this delay, negative-strand RNA accumulation in these cells did not plateau at 6 to 8 h p.i. as in wt-infected cells, but instead, RNA continued to accumulate through 20 h p.i. Moreover, as noted above for Fig. 2, the PK1 mutation reduced both positive- and negative-strand RNA1 accumulation relative to that of RNAs 2 and 3 (Fig. 3 and 4). PK1-infected cells shifted to 35°C at 4, 6, 8, and 10 h p.i. continued to accumulate positive-strand RNA. For cells shifted to 35°C at 2 h p.i., long exposure of the autoradiogram shown in Fig. 3 showed that accumulation of RNA was barely detectable and was equivalent to the low level seen for cells incubated continuously at 35°C. Additional negative-strand RNA accumulation occurred in aliquots shifted at 4 and 6 h p.i. but not in aliquots shifted at 8 and 10 h p.i.

TABLE 2. Direct-label analysis of temperature shift experiments

Inoculant[a]	Incubation conditions[b]	cpm[c]	
		Expt 1	Expt 2
Mock	A	35	37
	B	36	37
WT	A	68,906	98,477
	B	14,401	38,120
	C	54,615	70,993
	D	10,401	28,005
PK19	A	41,664	61,590
	B	32	45
	C	33,550	40,064
	D	36	48

[a] Mock, water only; WT, wt BMV RNAs 1 to 3; PK19, wt BMV RNAs 2 and 3 plus insertion mutant PK19.

[b] A and B, 20 h at 24 and 35°C, respectively, with continuous labeling with [5,6-^{3}H]uridine; C, 20 h at 24°C with labeling from 7 to 20 h; D, 6 h at 24°C and then 14 h at 35°C with labeling from 7 to 20 h p.i.

[c] ^{3}H-labeled RNA from approximately 3×10^4 inoculated protoplasts was hybridized with 10 μg of denatured plasmid pB3TP8 fixed onto nylon membranes as described in Materials and Methods. After hybridization, nonspecifically bound RNA was removed by washing and the amount of bound RNA was determined by liquid scintillation counting. Experiments 1 and 2 were independent inoculations.

In vivo labeling following temperature shift. To determine whether the absence of additional RNA accumulation in PK19-infected cells following the shift to 35°C is due to blockage of further synthesis or an altered balance of synthesis and degradation, direct labeling experiments were performed. For these experiments, cells were inoculated as described above and incubated for 6 h at 24°C prior to the shift to 35°C. After cells were allowed to equilibrate at the nonpermissive temperature for 1 h, [^{3}H]uridine was added, and incubation continued for an additional 13 h, for a total incubation time of 20 h. After total RNA was isolated, the extent of ^{3}H incorporation into viral RNA was determined by filter hybridization to denatured BMV RNA3 plasmid pB3TP8 as described in Materials and Methods. The results (Table 2) confirm that, as previously observed, wt-infected cells continued to synthesize RNA after the temperature shift. Since nearly equivalent positive-strand levels were seen by Northern blot analysis of wt-infected cells incubated at 24 and 35°C, the three- to fourfold reduction in [^{3}H]RNA levels in wt infections at 35°C compared with those at 24°C may reflect differential uptake of label by cells at the two temperatures. In contrast to wt-infected cells, PK19-infected cells showed no viral RNA synthesis after the shift to 35°C. This confirms that RNA detected by Northern blot analysis in cells shifted to 35°C (Fig. 3) represents RNA synthesized at 24°C prior to the shift and that prior synthesis of the PK19 1a protein at 24°C does not protect it from thermal inactivation.

Intragenic complementation tests. Complementation experiments were used to explore the possible multifunctional nature of the 1a protein. Initial experiments were performed with lethal mutants because of their distribution throughout the 1a protein. The number of inoculations needed to transfect protoplasts with all possible combinations of lethal RNA1 mutants was reduced by assigning mutants to four groups of three (A, B, C, and D; Fig. 1). Protoplasts were inoculated with wt RNAs 2 and 3, plus each individual mutant group, and with all possible pairs (A + B, A + C, etc.). If detectable RNA accumulation had occurred for any mixture of lethal mutants, additional inoculations performed with pairs of lethal mutants from the complementing groups would have identified the complementing RNAs. The results show, however, that no combination of lethal mutants directed detectable levels of RNA accumulation (Fig. 5A). Rather, the RNA levels seen in the long exposure of Fig. 5A are equivalent to the residual input inoculum levels seen when one or more components are omitted from the inoculation (see leftmost six lanes). Cells inoculated with each group of lethal mutants plus wt RNA1 show that BMV RNA accumulation is nearly identical to RNA accumulation in standard wt inoculations, even when the ratio of lethal to wt RNA1 is 6 to 1 (Fig. 5B).

Complementation tests were also performed at 35°C with *ts* mutant PK19 and selected lethal mutants with insertions in the N-terminal conserved domain (PK6, PK7, PK12, and

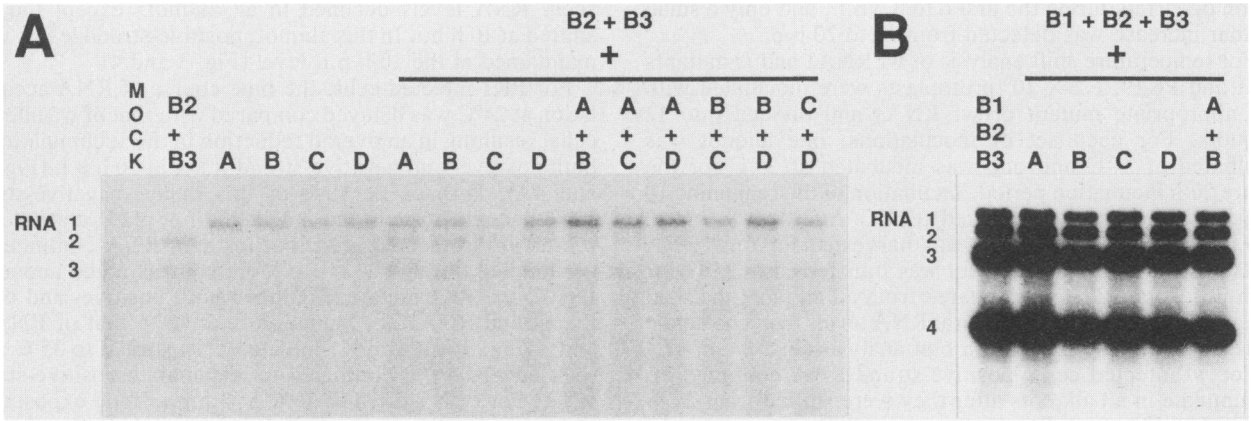

FIG. 5. Complementation tests between BMV RNA1 lethal mutants. Protoplasts were inoculated with mixtures of wt and lethal-mutant transcripts as indicated above each lane and incubated at 24°C for 20 h. Positive-strand RNA accumulation was determined by Northern blot techniques as described in Materials and Methods. B1, B2, and B3 represent transcripts from wt cDNA clones of BMV RNAs 1, 2, and 3, respectively, and A, B, C, and D represent mixtures of lethal-mutant transcripts as identified in the legend to Fig. 1. The mock lane contains RNA from protoplasts inoculated with water only. Autoradiograms are from the same experiment but were exposed for 8.5 days (A) and 0.5 days (B).

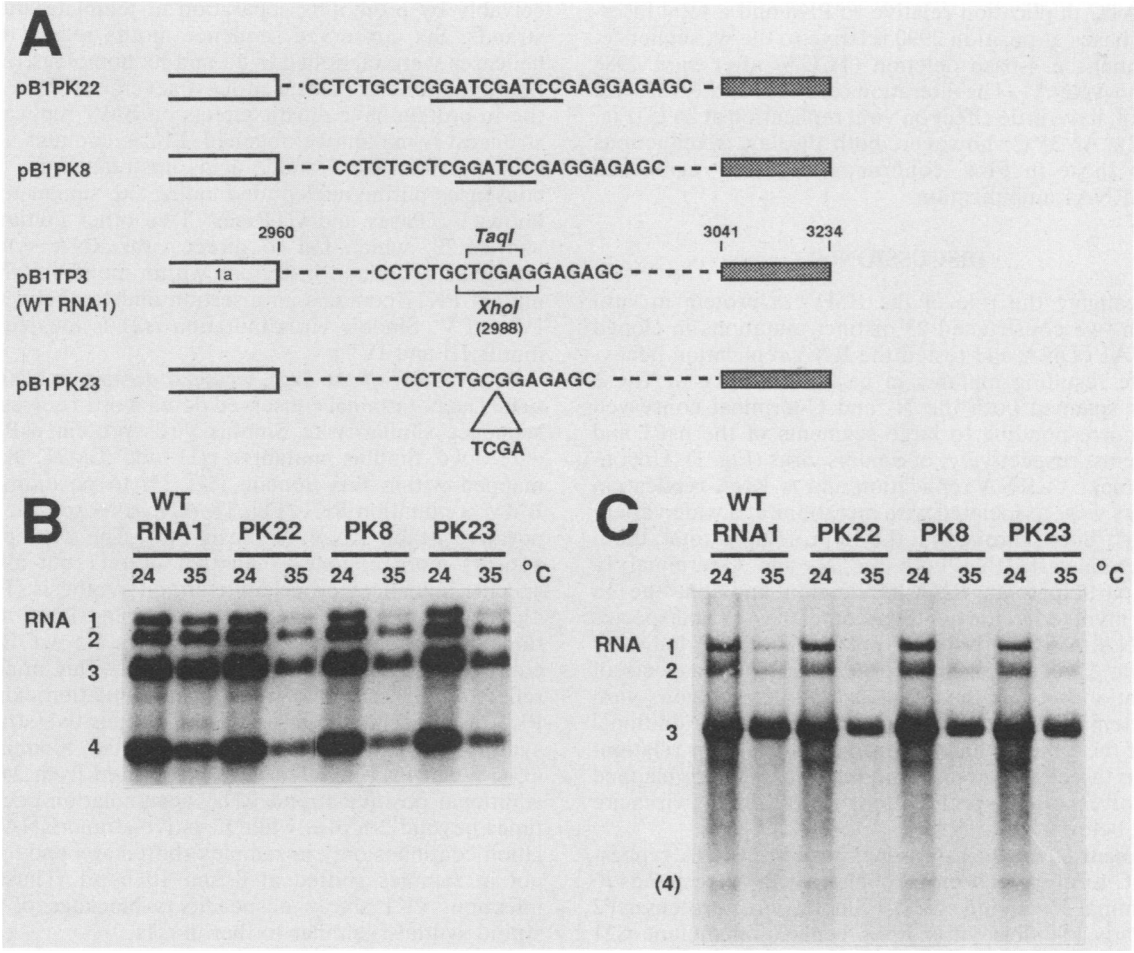

FIG. 6. Effects of mutations in the RNA1 3′ noncoding region on BMV replication in protoplasts. (A) Bases inserted or deleted in the 3′ noncoding region of BMV RNA1 in mutants PK8, PK22, and PK23. The open box represents the C-terminal portion of the 1a open reading frame, which ends at nucleotide 2960. The shaded box represents the sequence at the 3′ end of RNA1 (nucleotides 3041 to 3234) that is conserved among all BMV RNAs (3). Brackets identify the recognition sequences for the restriction enzymes utilized in the mutagenesis as described in the text. For PK8 and PK22, the nucleotides inserted into RNA1 are underlined, and for PK23, the triangle identifies the nucleotides deleted from RNA1. (B and C) Protoplasts were inoculated with transcripts from cDNA clones corresponding to wt RNA1 or mutants PK8, PK22, or PK23 plus transcripts from wt cDNA clones of RNAs 2 and 3. After incubation at 24 or 35°C for 20 h, total RNA was isolated and the levels of viral positive-strand (B) and negative-strand (C) RNA accumulation were determined by Northern blot techniques as described in Materials and Methods.

PK13) and, conversely, with *ts* mutant PK1 and selected lethal mutants from the C-terminal conserved domain (PK15, PK17, PK18, and PK20). As with the lethal mutant combinations alone, none of the PK19–lethal-mutant pairs showed detectable replication, and none of the PK1–lethal-mutant pairs showed replication greater than that observed in cells inoculated with PK1 alone (results not shown). Additionally, the same results were obtained in protoplasts incubated at 35°C after inoculation with all possible pair combinations of *ts* mutants PK1, PK4, and PK19 (results not shown).

Insertions in the 3′ noncoding region of RNA1. Mutant PK8 displays a *ts* replication defect due to a 6-nucleotide insertion 30 bases downstream from the 1a protein stop codon and 244 bases from the RNA1 3′ end (Table 1 and Fig. 6). At 24°C, this mutation has little effect on positive- or negative-strand RNA levels and does not detectably alter the ratio of individual RNAs (Fig. 6). When PK8-infected cells are incubated at 35°C, however, positive-strand RNA accumulation is reduced about twofold, with RNA1 levels showing an additional reduction of about twofold compared with the other RNAs (Fig. 6B). Similar decreases in negative-strand RNA accumulation were observed at 35°C (Fig. 6C).

To confirm the phenotype of PK8 and to ensure that this mutant did not contain an additional mutation in the 1a protein, the *Afl*II-*Eco*RI fragment of pB1PK8 was exchanged with the corresponding fragment from the wt RNA1 plasmid pB1TP3. This fragment contains the 3′-terminal 408 bases of RNA1, including the last 43 codons of the 1a gene. Sequence analysis of the entire fragment confirmed that the only alteration was the insertion of 6 bases at position 2990. Analysis of protoplasts inoculated with transcripts from the reconstructed clones showed that the PK8 phenotype was transferred to the wt clone and that PK8 reverted to wt after receiving the wt fragment.

To further analyze the ability of this region to influence BMV replication, two additional mutations were made at the position of the PK8 insertion (Fig. 6A). PK22 contains a

4-base GATC duplication relative to PK8 and a total insertion of 10 bases at position 2990 relative to the wt sequence. PK23 contains a 4-base deletion (TCGA) after base 2988 relative to wt RNA1. The alterations in PK22 and PK23, like that in PK8, have little effect on viral replication at 24°C (Fig. 6B and C). At 35°C, however, both display *ts* reductions similar to those in PK8, confirming that this region can influence RNA1 amplification.

DISCUSSION

To investigate the role of the BMV 1a protein in viral replication, we constructed 23 distinct mutations in cloned BMV RNA1 cDNA and tested the RNA replication behaviors of the resulting mutants in barley protoplasts. These mutations spanned both the N- and C-terminal conserved domains corresponding to large segments of the nsP1 and nsP2 proteins, respectively, of Sindbis virus (Fig. 1). Unconditional blocks to RNA replication and *ts* RNA replication phenotypes were associated with mutations at a wide variety of sites distributed throughout the 1a protein. In total, these results demonstrate that both the N- and C-terminal 1a domains participate in RNA replication and that the 1a protein is involved in the synthesis of all classes and species of viral RNA. A separate study from our laboratory indicates further that 1a is responsible for at least some aspects of discrimination between homologous and heterologous viral RNAs in template selection for replication (43). Additional aspects of the 1a insertion mutant results and their relationship to the three RNA replication mutants recently mapped into the corresponding protein domains of Sindbis virus are discussed below.

Involvement of the 1a C-terminal domain in RNA replication. The C-terminal conserved domain of 1a corresponds to the N-terminal 460 amino acids of Sindbis virus protein nsP2 (6). Recently, Sindbis virus RNA replication mutant *ts*21 was mapped within this region (17). The site of *ts*21 corresponds to a BMV 1a position between *ts* mutant PK19 and lethal mutant PK17 (Fig. 1). *ts*21 has a conditional defect only in subgenomic RNA synthesis (39). By contrast, when the strongly *ts* BMV 1a mutant PK19 is shifted from 24 to 35°C, synthesis of positive-strand, negative-strand, and subgenomic RNAs is blocked (Fig. 2 to 4; Table 2). Thus, whether because of multifunctionality or not, this intervirally conserved domain influences the synthesis not only of subgenomic RNA but also of all forms of genomic RNA. Consistent with this conclusion, antibodies to the C terminus of 1a inhibit de novo synthesis of BMV negative-strand RNA by BMV polymerase extracts prepared from infected plants (22, 35).

The C-terminal conserved domain of 1a protein contains extended sequence similarity to a number of nucleic acid helicases (16, 21). Helicase activity or activities, which might be virus or host encoded, seem likely to be required at several steps in BMV replication. In keeping with the antibody results described above, for example, RNA unwinding should greatly facilitate initiation of negative-strand RNA synthesis at the aminoacylatable 3' ends of BMV genomic RNAs, which bear extensive and highly stable secondary and tertiary structures (2). In addition, the observed ability of a BMV RNA polymerase extract to copy through template regions made double stranded by annealing to defined cDNAs suggests that substantial strand-separating activity is associated with elongation in BMV replication (1). This activity might normally assist elongation of RNA synthesis by unwinding template secondary structure or conceivably by promoting separation of template and nascent strands. Six conserved sequence motifs related to known helicases were identified in 1a and its homologs (21). Insertion mutations in or near at least several of these motifs in the 1a protein have drastic effects on BMV replication. The strongest *ts* mutant we obtained, PK19, contains a 2-amino-acid insertion just 9 amino acids upstream from motif I, a consensus purine nucleotide-binding site similar to those of known ATPases and GTPases. Two other mutants, PK18 and PK20, which fail to direct viral RNA synthesis in protoplasts, contain insertions within motif V, while lethal mutant PK17 contains an insertion midway between motifs IV and V. Sindbis virus mutation *ts*21 is located between motifs III and IV.

Involvement of the 1a N-terminal domain in RNA replication. The N-terminal conserved domain of 1a corresponds by sequence similarity to Sindbis virus protein nsP1 (6). To date, two Sindbis mutants, *ts*11 and LM21, have been mapped within this domain (17, 33) to positions flanking BMV *ts* mutation PK1 (Fig. 1). *ts*11 has a specific defect in negative-strand RNA synthesis (40). The PK1 phenotype appears more complex than that of *ts*11 but also shows specific influences on negative-strand synthesis (Fig. 3 and 4). At 24°C, PK1-directed negative-strand RNA accumulation does not plateau by 8 h p.i., as for wt BMV, but continues to increase through 20 h p.i. This might simply reflect the overall delay in RNA accumulation exhibited by PK1 or a specific defect in shutoff of negative-strand RNA synthesis, as has been observed for certain Sindbis mutants (39). When PK1-infected cells are shifted from 24 to 35°C, additional positive-strand RNA accumulation occurs at all times beyond 2 h p.i., while negative-strand RNA accumulation continues only in samples shifted at 4 and 6 h p.i. but not in samples shifted at 8 and 10 h p.i. Thus, later in infection, PK1 shows a specific *ts* blockage of negative-strand synthesis similar to that in *ts*11.

Sindbis mutation LM21 alters a virus-specific guanine-7-methyltransferase activity likely to be involved in viral RNA capping (33, 41). The positive-strand RNAs of BMV, Sindbis virus, and other members of the alphaviruslike superfamily all bear singly methylated m^7GpppN- caps, and it has previously been suggested that BMV 1a may encode methyl- and/or guanylyl-transferase activities involved in capping (13). Since it is not clear how a capping defect would alter negative-strand synthesis in the ways seen in BMV mutant PK1 and Sindbis mutant *ts*11, the N-terminal 1a-nsP1 domain may be multifunctional, or the phenotypic effects of some of the mutations described above may be indirect.

Complementation results. No detectable rescue of viral replication was seen with any of the possible combinations of the BMV 1a lethal mutants or with selected combinations of lethal and *ts* mutants incubated at 35°C. The inability of these mutants to complement one another suggests that a 1a function required for one or more stages of replication might depend on direct interaction of the N- and C-terminal domains. In keeping with such a possibility, all members of the alphaviruslike superfamily express the corresponding protein domains within a single covalently linked protein at some point in the infection (6, 18). Alternatively, the two 1a domains may carry out biochemically distinct functions but require close physical proximity because of temporal or topological limitations. For example, the results noted above suggest that the two 1a domains might provide functions involved in elongation of RNA synthesis and capping of product RNA. Such an association does occur in vaccinia virus transcription, in which virus-encoded RNA elongation

and capping activities appear to be complexed (9). Possible action of 1a in capping might then depend on the ability of the appropriate 1a domain to directly interact with the newly synthesized 5′ end of the nascent transcript as it is released from the elongation complex, prior to further elongation and RNA folding. The 5′ ends of full-length BMV RNAs 1 and 2 are in fact very poorly accessible to enzymes such as the vaccinia virus guanylyl-transferase (3).

While complementation between BMV mutants in the N- and C-terminal 1a domains was not observed, complementation between Sindbis virus mutants *ts*11 and *ts*21 is detectable but inefficient, producing only around 2% of the wt virus yield at 40°C (17). Although low, an equivalent level of complementation would have been easily detected in our BMV experiments, since the Northern blotting techniques used detect viral replication at or below 0.2% of wt levels. The ability to achieve low-level complementation between these Sindbis mutants, in contrast to our BMV results, may reflect the processing of nsP1 and nsP2 to individual proteins as well as to linked forms (18, 19). The potential for exchange of such proteins between coinfecting alphaviruses or the function of the final processed forms is still apparently limited, since inefficient complementation is typical for Sindbis virus mutants (10, 11, 42).

Influence of the 3′ noncoding region on RNA1 replication. While the last 134 bases of BMV RNA are necessary and sufficient in vitro to direct efficient negative-strand RNA synthesis (34), a larger 3′ region, corresponding approximately to the 200-base region highly conserved on all BMV RNAs (2), is required in vivo for high-level replication of BMV RNA3 (14). *ts* mutants PK8, PK22, and PK23 show that noncoding sequences upstream of the highly conserved 3′-terminal 200 bases of BMV RNAs can also influence RNA replication in vivo. Because these mutations occur in noncoding sequences, their primary effects are presumably *cis* acting, while their *trans*-acting effects are presumably mediated by a reduction in the level of RNA1 and consequent underproduction of 1a protein. The negative *trans*-acting effects of these mutations on RNA accumulation are relatively small but are still noteworthy because they result from only slight reductions in RNA1 levels. In contrast, significant viral RNA accumulation occurs in protoplasts containing only low levels of poorly replicating (37, 43) or nonreplicating (36; P. Kroner, M. Janda, and P. Ahlquist, unpublished results) RNA2 transcripts. An excellent example is provided by RNA2 mutant BC2PT15, whose accumulation is dramatically depressed in *cis* with only minor *trans*-acting effects (43). Thus, BMV RNA replication seems more sensitive to reductions in 1a mRNA levels than 2a mRNA levels, and while less 2a than 1a protein appears to be required, 1a expression may be close to a limiting step in BMV replication. In keeping with these observations, a translational readthrough mechanism in tobacco mosaic virus ensures that the protein domains corresponding to BMV 1a are substantially overexpressed relative to the protein domain analogous to BMV 2a. An engineered tobacco mosaic virus mutant in which the relevant wt amber readthrough termination codon was replaced by a sense codon propagated slowly and was overgrown by a pseudorevertant bearing an ochre readthrough termination codon (24). Sindbis virus incorporates both translational readthrough and processing mechanisms that contribute to maintaining a corresponding asymmetric balance of the analogous nonstructural proteins (31).

ACKNOWLEDGMENTS

We thank Patricia Traynor, Douglas Richards, and Radiya Pacha for helpful discussions during the course of these experiments.

This work was supported by Public Health Service grant GM35072 from the National Institutes of Health.

LITERATURE CITED

1. **Ahlquist, P., J. J. Bujarski, P. Kaesberg, and T. C. Hall.** 1984. Localization of the replicase recognition site within brome mosaic virus RNA by hybrid-arrested RNA synthesis. Plant Mol. Biol. **3**:37–44.
2. **Ahlquist, P., R. Dasgupta, and P. Kaesberg.** 1981. Near identity of 3′ RNA secondary structure in bromoviruses and cucumber mosaic virus. Cell **23**:183–189.
3. **Ahlquist, P., R. Dasgupta, and P. Kaesberg.** 1984. Nucleotide sequence of the brome mosaic virus genome and its implications for viral replication. J. Mol. Biol. **172**:369–383.
4. **Ahlquist, P., R. French, M. Janda, and L. S. Loesch-Fries.** 1984. Multicomponent RNA plant virus infection derived from cloned viral cDNA. Proc. Natl. Acad. Sci. USA **81**:7066–7070.
5. **Ahlquist, P., V. Luckow, and P. Kaesberg.** 1981. Complete nucleotide sequence of brome mosaic virus RNA3. J. Mol. Biol. **153**:23–38.
6. **Ahlquist, P., E. G. Strauss, C. M. Rice, J. H. Strauss, J. Haseloff, and D. Zimmern.** 1985. Sindbis virus proteins nsP1 and nsP2 contain homology to nonstructural proteins from several RNA plant viruses. J. Virol. **53**:536–542.
7. **Barany, F.** 1985. Two codon insertion mutagenesis of plasmid genes by using single-stranded hexameric oligonucleotides. Proc. Natl. Acad. Sci. USA **82**:4202–4206.
8. **Barton, D. J., S. G. Sawicki, and D. L. Sawicki.** 1988. Demonstration in vitro of temperature-sensitive elongation of RNA in Sindbis virus mutant *ts*6. J. Virol. **62**:3597–3602.
9. **Broyles, S., and B. Moss.** 1987. Sedimentation of an RNA polymerase complex from vaccinia virus that specifically initiates and terminates transcription. Mol. Cell. Biol. **7**:7–14.
10. **Burge, B. W., and E. R. Pfefferkorn.** 1966. Isolation and characterization of conditional-lethal mutants of Sindbis virus. Virology **30**:204–213.
11. **Burge, B. W., and E. R. Pfefferkorn.** 1966. Complementation between temperature-sensitive mutants of Sindbis virus. Virology **30**:214–230.
12. **Cornelissen, B., and J. Bol.** 1984. Homology between proteins encoded by tobacco mosaic virus and two tricornaviruses. Plant Mol. Biol. **3**:379–384.
13. **Dreher, T. W., and T. C. Hall.** 1988. RNA replication of brome mosaic virus and related viruses, p. 91–113. *In* E. Domingo, J. J. Holland, and P. Ahlquist (ed.), RNA genetics. CRC Press, Inc., Boca Raton, Fla.
14. **French, R., and P. Ahlquist.** 1987. Intercistronic as well as terminal sequences are required for efficient amplification of brome mosaic virus RNA3. J. Virol. **61**:1457–1465.
15. **Goldbach, R.** 1987. Genome similarities between plant and animal RNA viruses. Microbiol. Sci. **4**:197–202.
16. **Gorbalenya, A. E., and E. V. Koonin.** 1989. Viral proteins containing the purine NTP-binding sequence pattern. Nucleic Acids Res. **17**:8413–8440.
17. **Hahn, Y. S., E. G. Strauss, and J. H. Strauss.** 1989. Mapping of RNA$^-$ temperature-sensitive mutants of Sindbis virus: assignment of complementation groups A, B, and G to nonstructural proteins. J. Virol. **63**:3142–3150.
18. **Hardy, W. R., and J. H. Strauss.** 1988. Processing the nonstructural polyproteins of Sindbis virus: study of the kinetics in vivo by using monospecific antibodies. J. Virol. **62**:998–1007.
19. **Hardy, W. R., and J. H. Strauss.** 1989. Processing the nonstructural polyproteins of Sindbis virus: nonstructural proteinase is in the C-terminal half of nsP2 and functions both in *cis* and in *trans*. J. Virol. **63**:4653–4664.
20. **Haseloff, J., P. Goelet, D. Zimmern, P. Ahlquist, R. Dasgupta, and P. Kaesberg.** 1984. Striking similarities in amino acid sequence among nonstructural proteins encoded by RNA viruses that have dissimilar genomic organization. Proc. Natl. Acad. Sci. USA **81**:4358–4362.

21. **Hodgman, T. C.** 1988. A new superfamily of replicative proteins. Nature (London) **333**:22–23. (Erratum, **333**:578.)
22. **Horikoshi, M., K. Mise, I. Furusawa, and J. Shishiyama.** 1988. Immunological analysis of brome mosaic virus replicase. J. Gen. Virol. **69**:3081–3087.
23. **Inokuchi, Y., and A. Hirashima.** 1987. Interference with viral infection by defective RNA replicase. J. Virol. **61**:3946–3949.
24. **Ishikawa, M., T. Meshi, F. Motoyoshi, N. Takamatsu, and Y. Okada.** 1986. In vitro mutagenesis of the putative replicase genes of tobacco mosaic virus. Nucleic Acids Res. **14**:8291–8305.
25. **Janda, M., R. French, and P. Ahlquist.** 1987. High efficiency T7 polymerase synthesis of infectious RNA from cloned brome mosaic virus cDNA and effects of 5′ extensions on transcript infectivity. Virology **158**:259–262.
26. **Kamer, G., and P. Argos.** 1984. Primary structural comparison of RNA-dependent polymerases from plant, animal, and bacterial viruses. Nucleic Acids Res. **12**:7269–7282.
27. **Kiberstis, P., L. S. Loesch-Fries, and T. C. Hall.** 1981. Viral protein synthesis in barley protoplasts inoculated with native and fractionated brome mosaic virus RNA. Virology **112**:804–808.
28. **Kroner, P., D. Richards, P. Traynor, and P. Ahlquist.** 1989. Defined mutations in a small region of the brome mosaic virus 2a gene cause diverse temperature-sensitive RNA replication phenotypes. J. Virol. **63**:5302–5309.
29. **Laemmli, U. K.** 1970. Cleavage of structural proteins during the assembly of the head of bacteriophage T4. Nature (London) **227**:680–685.
30. **Lane, L.** 1981. Bromoviruses, p. 333–376. *In* E. Kurstak (ed.), Handbook of plant virus infections and comparative diagnosis. Elsevier/North Holland Biomedical Press, Amsterdam.
31. **Li, G., and C. M. Rice.** 1989. Mutagenesis of the in-frame opal termination codon preceding nsP4 of Sindbis virus: studies of translational readthrough and its effect on virus replication. J. Virol. **63**:1326–1337.
32. **Maniatis, T., E. F. Fritsch, and J. Sambrook.** 1982. Molecular cloning: a laboratory manual. Cold Spring Harbor Laboratory, Cold Spring Harbor, N.Y.
33. **Mi, S., R. Durbin, H. V. Huang, C. M. Rice, and V. Stollar.** 1989. Association of the Sindbis virus RNA methyltransferase activity with the nonstructural protein nsP1. Virology **170**:385–391.
34. **Miller, W. A., J, J. Bujarski, T. W. Dreher, and T. C. Hall.** 1986. Minus-strand initiation by brome mosaic virus replicase within the 3′ tRNA-like structure of native and modified RNA templates. J. Mol. Biol. **187**:537–546.
35. **Quadt, R., H. J. M. Verbeek, and E. M. J. Jaspers.** 1988. Involvement of a nonstructural protein in the RNA synthesis of brome mosaic virus. Virology **165**:256–261.
36. **Rao, A. L. N., and T. C. Hall.** 1990. Requirement for a viral *trans*-acting factor encoded by brome mosaic virus RNA-2 provides strong selection in vivo for functional recombinants. J. Virol. **64**:2437–2441.
37. **Sacher R., R. French, and P. Ahlquist.** 1988. Hybrid brome mosaic virus RNAs express and are packaged in tobacco mosaic virus coat protein in vivo. Virology **167**:15–24.
38. **Sawicki, D. L., D. B. Barkhimer, S. G. Sawicki, C. M. Rice, and S. Schlesinger.** 1990. Temperature-sensitive shut-off of alphavirus minus strand RNA synthesis maps to a nonstructural protein, nsP4. Virology **174**:43–52.
39. **Sawicki, D. L., and S. G. Sawicki.** 1985. Functional analysis of the A complementation group mutants of Sindbis HR virus. Virology **144**:20–34.
40. **Sawicki, D. L., S. G. Sawicki, S. Keränen, and L. Kääriäinen.** 1981. Specific Sindbis virus-coded function for minus-strand RNA synthesis. J. Virol. **39**:348–358.
41. **Scheidel, L. M., R. K. Durbin, and V. Stollar.** 1989. SV_{LM21}, a Sindbis virus mutant resistant to methionine deprivation, encodes an altered methyltransferase. Virology **173**:408–414.
42. **Strauss, E. G., E. M. Lenches, and J. H. Strauss.** 1976. Mutants of Sindbis virus. I. Isolation and partial characterization of 89 new temperature-sensitive mutants. Virology **74**:154–168.
43. **Traynor, P., and P. Ahlquist.** 1990. Use of bromovirus RNA2 hybrids to map *cis*- and *trans*-acting functions in a conserved RNA replication gene. J. Virol. **64**:69–77.